Dependence of the specific surface area of the nuclear fuel with the matrix oxidation

F. Gómez, J. Quiñones, E. Iglesias, N. Rodriguez

CIEMAT. Avda. Complutense 22, 28040-Madrid.SPAIN.
javier.quinones@ciemat.es

Abstract –*This paper is focused on the study of the changes in the specific surface area measured using BET techniques. The objective is to obtain a relation between this parameter and the change in the matrix stoichiometry (i.e., oxidation increase).None of the actual models used for extrapolating the behaviour of the spent fuel matrix under repository conditions have included this dependence yet.*
In this work the specific surface area of different uranium oxide were measured using N_2(g) and Kr(g). The starting material was UO_{2+x}(s) with a size powder distribution lower than 20 µm. The results included in this paper shown a strong dependence on specific surface area with the matrix stoichiometry, i.e., and increase of more than one order of magnitude (S_{UO2} = 6 $m^2 \cdot g^{-1}$ and S_{U3O8} = 16.07 $m^2 \cdot g^{-1}$). Furthermore, the particle size distribution measured as a function of the thermal treatment done shows changes on the powder size related to the changes observed in the uranium oxide stoichiometry

INTRODUCTION

One of the key issues in the performance assessment studies is to model and extrapolate the alteration behavior of the spent fuel under repository conditions. The environmental conditions considered in this paper are based on the following scenario: the groundwater surrounding the spent fuel pellet in a deep geological disposal is in reducing conditions due to host rock chemical composition [1].
A hypothetical containers failure would allow the water to get in touch with UO_2 fuel pellet. As consequence of its high-intensity radiation field, radiolysis reaction of water will take place, eventually changing water conditions from reducing to oxidizing, and thus, increasing UO_2 oxidation state [2, 3]. This fact would have a relevant role in safety analysis of geological disposal because a great increase in dissolution rate of uranium oxides happens after a evolution to oxidizing conditions [2, 4-6].
Focused on the spent fuel alteration process there are a few key variables that control the kinetics of the alteration process, i.e, temperature, partial pressure of hydrogen, groundwater composition, initial oxidation state of the matrix, specific surface area, etc. The experimental work presented in this paper is based on previous studies performed by some of the authors [7-9] using the Matrix Alteration Model [8, 9] as a powerful tool to extrapolate to relevance times for PA studies of the spent fuel behavior under repository conditions. The sensitivity analysis of the MAM model [9] points out that the specific surface area of the matrix will play relevant role on the final dissolution rate observed.
Furthermore it is well known that the surface oxidation state of the matrix has a key influence on the initial dissolution rates obtained [3, 7, 10].
Taking into account the aforementioned uncertainties, this work has been focused on the dependence of the specific surface area variation with the oxidation state of UO_{2+x}. If some change were observed this fact will have a strong influence on the spent fuel matrix stability under repository conditions, due to the modification of the alteration rate of the matrix (as explained in the MAM) [8, 9].

EXPERIMENTAL PROCEDURE

The base material used in this experimental work was a UO_2 sintered pellet supplied by ENUSA. The pellet were crushed and sieved in order to obtain an homogeneous distribution of the particle size lower than 20 µm.
To broach this topic, a set of samples with different oxidation degree has been prepared, with an O/U ratio ranging from 2 to 8/3 [6, 11, 12]. These samples have been processed by a thermo chemical treatment in a muffle furnace after making several tests related to oxidation kinetics working with thermogravimetical methods. The oxygen content in the experimental atmosphere air is important as it controls the reaction kinetics, as the temperature do.
The sample preparation have not been carried out with oxygen content control neither high-vacuum conditions; this means that experimental conditions are far from equilibrium [13]. This

leads to a displacement of the reaction in the sense of oxidized products formation.
For the bulk analysis, a Philips XRD X'PERT-MPD model was used. To avoid the optical aberrations, the characterization of a Si pattern was performed, correcting the displacement to get the best fit from the signs obtained with this test pattern and the peaks from JCPDS archives [14].
The characterization method used to evaluate the specific surface area of the UO_x samples has been the BET technique [15], performed in a chemical-physical adsorption equipment (ASAP 2020-MICROMERITICS) using N_2 and Kr as vapour "adsorbat" in a physical adsorption-desorption loop over UO_{2+x} adsorbent.
To obtain a value for the specific surface area of a sample, the equipment makes a gas flow to circulate and pass through the sample. A process of adsorption will take place in its surface, controlling the pressure conditions (P/P_0).
A linear regression of the data obtained allows to calculate BET area.
The experiments have been carried out at constant temperature (boiling temperature of nitrogen at atmospheric pressure: 77 K) in order to keep constant equilibrium conditions. In these context, the BET theory gives equilibrium isotherm for adsorption [15]

$$q_e = \frac{B\,P\,q_m}{\left(P_0 - P\right)\left[1 + (B-1)\left(P/P_0\right)\right]} \qquad (1)$$

Linear form of this equation permits to calculate adsorption parameters and work with these results:

$$\frac{P}{\left(P_0 - P\right)q_e} = \frac{1}{B\,q_m} + \frac{P}{P_0}\left(\frac{B-1}{B\,q_m}\right) \qquad (2)$$

Samples prepared have been measured in order to determine their oxidation states. As consequence of this dry oxidation due to high temperature, several UO_x non-stoichiometric phases appear: UO_{2+x}, U_4O_{9+x} and U_3O_{8-x}. The degree of mixing among these phases will be given by thermal treatment (heating rate, time and temperature reached).
According to the thermal treatment and oxidation degree the samples prepared have been named as follows: i. Sample A: no heat treatment, ii. Sample B: 290 °C during 30 min, iii. Sample C: 290 °C during 1 h, iv. Sample D: 290 °C during 2 h, v. Sample E: 290 °C during 8 h, vi. Sample F: 1100 °C during 7 h, vii. Sample G: reduction of basis sample in H_2/N_2 atmosphere.
Moreover, samples with different heat treatment temperature will illustrate about influence of particle size distribution (highly influenced by thermal treatment) in samples specific surface with the same oxidation states and quite different heat treatments and how it works depending on the adsorbat that gets in touch with uranium oxide.
To characterize the UO_x particle size distribution has been determined by laser diffraction performed in a MALVERN 2600 and a sodium phosphate solution (0.5 $g \cdot dm^{-3}$). A comparative study of particle size variation has been carried out using UO_{2+x} particle size distribution between 0 and 20 μm (due to this small size this effect will be limited).

RESULTS AND DISCUSSION

The samples obtained and characterized by thermogravimetrical methods have been evaluated by X-ray diffraction and differential scanning calorimetry (DSC) to characterize the different oxidation states and phase transitions that have taken place.
The results obtained with this bulk characterization technique have been summarised in Fig. 1. The upper part of the Fig. 1 (DSC results) shows two different phase transitions, corresponding to the two-step oxidation aforementioned. However the lower plot of the Fig. 1 (TG data), illustrates a mass increase directly related to oxidation process (interstitial oxygen into oxide lattice sites). Form these results an empirical relation between O/U ratio vs time (thermal treatment, setting a constant temperature of 290 °C) have been propounded:

$$O/U = 2.13 + 5.43\times10^{-6}\ t/s \qquad (3)$$

Taking into account this results a set of different thermal treatment was performed in order to get uranium oxides with different O/U ratios (described on the experimental procedure).
A small amount of each sample were characterised by XRD, allowing to measure the modification on the lattice structure parameters and the level of oxidation achieved. The evolution of XRD-patterns as a function of the thermal treatment are seen in, Fig. 2.

Furthermore this plot shows the transition from UO_2 crystalline structure to U_3O_8 structure, as their respective peaks vanish and arise.

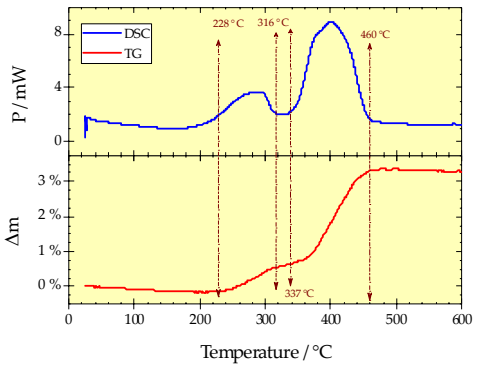

Fig. 1 TG and DSC data and phase transitions and oxidation process measured, using UO_2 sample (particle size distribution < 20 µm).

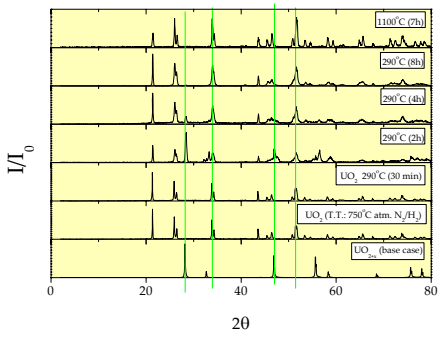

Fig. 2 XRD pattern obtained as a function of the thermo chemical treatment of the sample (oxidation state)

The samples A, B, C, D, E, F and G will show that BET surface increases as their oxidation degree (details from particle size due to heat treatment will be discussed later). However, sample C is not shown in Fig. 2 but the correlation between oxidation process and temperature is clear. Results from adsorption/desorption of nitrogen and krypton are quite different. This fact points out the necessity of not only mention the method used but also the gas used for the measurement. The differences between N_2 and Kr come from different radii and different affinities with uranium oxides (UO_{2+x}).

In general, the higher size of nitrogen molecule and reactivity results in an overestimation of the specific surface area. Grossly, because the amount of nitrogen than can be adsorbed over uranium oxide it is more than in the case of krypton.
Moreover, the heat treatment has a significant influence in the particle size distribution, which has a strong influence in the value of specific surface measured, due to the fragmentation process suffered by the sample during the thermal treatment (change on lattice structure). In this context, samples E and F will show this different behaviour in spite of having the same oxidation degree (U_3O_8).
As follows, the results from particle size distribution measurements are presented here showing how the temperature and time of the heat treatment affects this parameter (higher fragmentation is related to a decrease of the particle size distribution of the sample). However, the measurements done illustrate that this will not have the same effects in the case of nitrogen adsorption as in krypton adsorption.

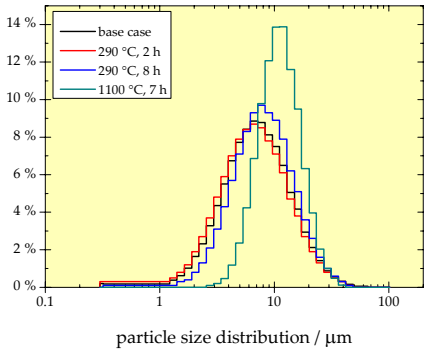

Fig. 3 Particle size distribution measured for simples A, D, E and F

The histogram distribution of each sample has been plotted in the Fig. 3. As it can be observed the particle size distribution changes as a consequence of the thermal treatment applied. If the base case measurement is compared to those samples treated, an increase of the lowest sizes and a decrease of the highest are observed. Furthermore, when the thermal treatment temperature is higher, a decrease of the lower sizes and an increase in the maximum size distribution is measured. This behaviour is explained by the volume increase resulting of the thermal treatment (oxidation process).

At first glance (see Fig. 3), lower sizes should dominate the distribution due to fragmentation of particles after dilatation as a consequence of tensile stresses that forces to rupture, but this effect can not be shown because the smaller size the faster dissolve on the liquid used during the measure. So, smallest particles dissolve and become not observable by the experimental device resulting in a higher percentage of bigger particles.
The rest of the samples measured are compiled in Fig. 4. It can be seen (by comparison to base material –sample A) that the temperature of the thermal treatment has an important role on the final particle size distribution obtained. As it was explained (Fig. 3) higher temperature (thermal treatment) induces a shift towards medium sizes, due to the reasons pointed out above, thermal expansion, oxidation, fracture of greater particles and dissolution of smaller ones.

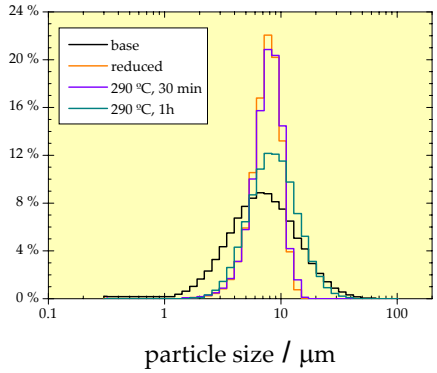

Fig. 4 Particle size distribution measured for samples A, B, C and G

The laser diffraction technique allows to define the particle size distribution of the sample as a function of 3 value (see Table I). These values correspond to the size value obtained for different % of the frequency distribution (i.e., 50, 10 and 90 %)
As it can be observed (Table I) using this type of size distribution definition not so high differences in the particle size are detected; with the traditional methods of sieving it can not be observed.
Regarding to the influence of the particle size distribution and oxidation state changes on the specific surface area would have an appreciable effect on this parameter. It is important to clarify to reader that in this paper, a discussion of the influence of the particle size on the surface area will be not included. It is focussed only on the influence of the matrix oxidation state.

Table I.- Particle size distribution vs thermal treatment applied

Sample	D[v,0.5] / µm	D[v,0.1] / µm	D[v,0.9] / µm
A (UO_{2+x})	8.13	3.47	19.06
D (290 °C, 2 h)	7.74	3.25	18.41
E (290 °C, 8 h)	9.24	4.24	20.16
F (1100 °C, 7 h)	12.77	7.44	21.90

The specific surface area measurements as a function of the O/U ratio are showed on Fig. 5. An increase of more than one order of magnitude in the specific surface area measured when the O/U ratio changes from 2 – 3 is observed.
The differences observed on the specific surface area for the same matrix oxidation state(U_3O_8, samples E & F) come from the different particle size distribution (see Table I), As can be seen in Fig. 5, BET surface values increase with oxidation degree. And, it can be seen that U_3O_8 sample has two quite different values of BET surface depending on the heat treatment. This behaviour is observed with both gases (N_2 and Kr). Samples treated with higher temperatures will show a major fragmentation and this fact can have a lot of different influences in the values experimentally obtained; as a strong variation in the quantity of gas that can be adsorbed over the oxide surface depending on the type of porosity generated due to the heat treatment. In turn, it is affected by chemical and physical reactivity of gas molecule, as well as by its size, etc, resulting in a very huge amount of small contributions that can lead to different tendencies in BET surface determination.
In this sense (Fig. 5) it can be observed how Kr gives quite lower BET area values, due to a less affinity for physical or chemical reacting of Kr with uranium oxide. This explains the lower quantity of Kr that can be adsorbed over sample surface.
Therefore, lower Kr affinity effect is dominant against lower size one, and its greater influence in BET surface area drives to lower BET area values than in N_2 case.
Since MAM [8, 9] does not consider specific surface area as a variable value but a constant, these results point out that it should be convenient to define exactly how this parameter

varies with oxidation state in order to quantify consequently dissolution rate variations, as specific surface area is a key parameter in this evaluation.

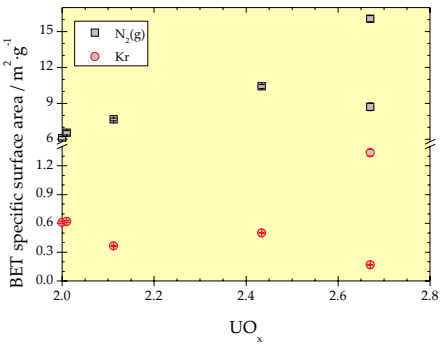

Fig. 5 Evolution of BET specific surface area measured as a function of the matrix oxidation state.

CONCLUSIONS

UO_{2+x} oxidation is a two-step process which shows the presence of three relevant species: UO_{2+x}, U_3O_7/U_4O_9 and U_3O_8.
UO_{2+x} is the most stable phase at low temperatures while U_3O_8 is the stable one at higher temperatures (thermogravimetical determination of oxidation kinetics shows that below 260 - 270 °C U_3O_8 formation does not take place). Moreover, this transformation has associated a volume increase of ≈ 37 % (which causes stresses and a significant loss of mechanical properties, which, joint with its higher dissolution rate compared with UO_{2+x}, justify the necessity of studying these parameters in order to characterize uranium oxide and its long term behaviour in deep geological disposal).
Particle size distribution of uranium oxides tends to have a higher proportion of middle sizes when a heat treatment is performed, due to a molar volume increase, which, in turn, leads to fragmentation, and also due to a much more rapid dissolution of smallest particles. Both effects contribute to decrease the proportion of the smallest and biggest particles detected by the equipment (whose limits have been defined prior to performing the experiments, between 0 and 20 μm).

The increase of BET specific surface with the oxidation state can have a great influence in the Matrix Alteration Model (MAM), as this magnitude is a determinant one in the dissolution rate which, until present time, it is considered to be constant. In general, both sets of experiments lead to an increase of BET specific surface area of a factor of 2-3.
Nitrogen adsorption leads to overestimation of specific surface area while krypton adsorption shows an underestimated one. Neither N_2 nor Kr adsorption can, by themselves, characterize the specific surface area of the sample but define boundary lines.
Hysteresis in desorption curve for krypton can have a relevant paper in underestimation of BET surface since a lower partial pressure is needed to reach to remove krypton gas from sample. As a consequence, the quantity of gas for a given partial pressure is higher in the desorption process than in the adsorption one.

ACKNOWLEDGEMENTS

This work has been financed by the following research projects: ACACIAS (Annexe VII from the CIEMAT-Enresa agreement d), and AMAME (Spanish R&D Program).

REFERENCES

[1] J. Astudillo Pastor, El almacenamiento geológico profundo de los residuos de alta actividad. Principios básicos y tecnología: ENRESA, 2001.
[2] J. Quiñones and J. Serrano, "Studies of the influence of water radiolysis to the spent fuel matrix dissolution process," in Hot Laboratories and Remote Handling, J. L. Díaz and J. Quiñones, Eds. Madrid: Ciemat, 2002.
[3] K. Spahiu, P. Carbol, J. Cobos, J. P. Glatz, C. Ronchi, V. V. Rondinella, D. Wegen, T. Wiss, A. Loida, V. Metz, B. Kienzler, B. Grambow, J. Quiñones, and A. Martínez Esparza, "The effect of dissolved hydrogen on the corrosion rates of 233U doped UO2(s), high burnup spent fuel and MOX fuel.," in Technical Report. vol. TR-05-09, K. Spahiu, Ed.: SKB, 2004, p. 63.
[4] L. H. Johnson, C. Poinssot, J. M. Cavedon, Z. Andriambololona, D. Wegen, B. Grambow, K. Spahiu, M. Kelm, H. Christensen, J. de Pablo, A. Martínez Esparza, J. Bruno, J. Quiñones, K. Lemmens, G. Mayer, C. Jegou, C. Ferry, P.

Lovera, A. Poulesquen, F. Miserque, C. Corbel, P. Carbol, J. P. Glatz, J. Cobos, D. Serrano, V. V. Rondinella, T. Wiss, V. Metz, A. Loida, B. Kienzler, T. Lundstrôm, M. Jonsson, I. Casas, M. Rovira, F. Clarens, J. A. Gago, E. Cera, J. Merino, A. González de la Huebra, E. Iglesias, and C. Cachoir, "Spent fuel evolution under disposal conditions. Synthesis of the results from the Eu Spent Fuel Stability (SFS) project." vol. 04-09 Wettingen: Nagra, 2005.

[5] J. Quiñones, J. Merino, E. Cera, J. Bruno, J. Cobos, and A. Martínez Esparza, A radiolytic modelling intercomparison exercise: Influence of alpha radiation on spent fuel alteration process. Oxford, England: American Society of Mechanical Engineers (ASME), 2003.

[6] C. Ferry, C. Poinssot, V. Broudic, C. Cappelaere, L. Desgranges, P. Garcia, C. Jegou, P. Lovera, P. Marimbeau, J. P. Piron, A. Poulesquen, D. Roudil, J.-M. Gras, and P. Bouffioux, "Synthesis on the spent fuel long term evolution," CEA, Saclay CEA-R-6084, june 2005.

[7] J. Quiñones, J. Cobos, P. P. Díaz Arocas, and V. V. Rondinella, "Modelling of the (U1-y238Puy)O2+x leaching behaviour in deionised water under anoxic conditions," in Scientific Basis for Nuclear Waste Management XXVII. vol. 807, V. M. Oversby and L. O. Werme, Eds.: Materials Research Society, 2004, pp. 409-414.

[8] A. Martínez Esparza, M. A. Cuñado, J. A. Gago, J. Quiñones, E. Iglesias, J. Cobos, A. González de la Huebra, E. Cera, J. Merino, J. Bruno, J. de Pablo, I. Casas, F. Clarens, and J. Giménez, "Development of a Matrix Alteration Model (MAM)," in Publicaciones técnicas. vol. 1-05: ENRESA, 2005.

[9] J. Quiñones, E. Iglesias, A. Martínez Esparza, J. Merino, E. Cera, J. Bruno, J. De Pablo, I. Casas, J. Giménez, F. Clarens, and M. Rovira, "Modelling of the spent fuel dissolution rate evolution for repository conditions. Matrix Alteration Model results and sensitivity analysis," in Scientific Basis for Nuclear Waste Management XXIX. vol. 932, P. V. Iseghem, Ed.: Material Research Society., 2006, pp. 433-440.

[10] C. Poinssot, C. Ferry, M. Kelm, B. Grambow, A. Martínez Esparza, L. Johnson, Z. Andriambololona, J. Bruno, C. Cachoir, J. M. Cavedon, H. Christensen, C. Corbel, C. Jegou, K. Lemmens, A. Loida, P. Lovera, F. Miserque, J. De Pablo, A. Poulesquen, J. Quiñones, V. V. Rondinella, K. Spahiu, and D. Wegen, Final report of the european project Spent Fuel Stability under repository conditions vol. CEA-R-6093. Saclay, 2005.

[11] J. Cobos, "Simulación de combustible nuclear de grado de quemado muy alto. Fabricación, caracterización y comportamiento a la oxidación," in Departamento de Ciencia de Materiales e Ingeniería Metalúrgica. Facultad de CC. Químicas Madrid: Universidad Complutense de Madrid, 1998, p. 326.

[12] J. A. Serrano, "Caracterización y lixiviación de combustibles nucleares irradiados y de sus análogos químicos," in Ciencia de Materiales e Ingeniería Metalúrgica: Universidad Complutense de Madrid, 2000, p. 300.

[13] J. D. Higgs, W. T. Thompson, B. J. Lewis, and S. C. Vogel, "Kinetics of precipitation of U4O9 from hyperstoichiometric UO2+x," J. Nucl. Mater., vol. 366, pp. 297-305, 2007.

[14] JCPDS - ICDD, "PCPDFWIN," 2.02 ed: International Centre for Diffraction Data, 1999.

[15] S. Brunauer, P. Emmet, and E. Teller, J. Am.Chem. Soc., vol. 60, p. 309, 1938.